Electronic Supplementary Information

PZT like structural phase transitions in the $BiFeO_3$-$KNbO_3$ solid solution

Robert C. Lennox,[a] Daniel. D. Taylor,[b] Laura J. Vera Stimpson,[a] Gavin B. G. Stenning,[c] Marek Jura,[c] Mark C. Price,[a] Efrain E. Rodriguez[d] and Donna C. Arnold[a*]

[a] *School of Physical Sciences, University of Kent, Canterbury, Kent, CT2 7NH, UK*

[b] *Department of Materials Science and Engineering, University of Maryland, College Park, MD, 20742-2115, USA.*

[c] *ISIS Neutron and Muon Source, Rutherford Appleton Laboratory, Harwell Science and Innovation Campus, Didcot, Oxon, Ox11 0QX, UK*

[d] *Department of Chemistry and Biochemistry, University of Maryland, College Park, MD 20742-4454, USA.*

[*] *Corresponding Author, Donna C. Arnold, e-mail: d.c.arnold@kent.ac.uk, tel: 01227 827810, fax: 01227 827558*

Experimental Details:

Room temperature time-of-flight powder neutron diffraction measurements were performed on the high resolution powder diffractometer (HRPD) at the ISIS facility, UK. Data were collected for materials in the $Bi_{1-x}K_xFe_{1-x}Nb_xO_3$ system with increasing compositional increments of $x = 0.10$ between $0.20 \leq x \leq 0.90$ and $Bi_{0.05}K_{0.95}Fe_{0.05}Nb_{0.95}$ with materials loaded into 6 mm diameter cylindrical vanadium cans. Room temperature synchrotron diffraction data were collected on the high resolution diffraction beamline (I11) at the Diamond Light Source, UK ($\lambda = 0.825659(2)$ Å and 2θ zero point = 0.0013917(3)). Data were collected with increasing compositional increments of $x = 0.10$ between $0.00 \leq x \leq 1.00$. In order to minimise absorption effects, associated with bismuth at the synchrotron radiation energy employed in these experiments and the glass capillaries used, samples were loaded onto the outside surface of 0.3 mm diameter glass capillaries by applying a thin layer of hand cream and rolling the capillary in the sample to provide an even coat of material. X-ray Fluorescence data was collected to probe the average composition of these materials using the PANalytical MiniPal4 spectrometer. Materials were prepared as pellets and analysis was performed taking into account the parent $BiFeO_3$ and $KNbO_3$ materials.

Room temperature Raman spectra were collected on powdered samples mounted onto aluminium sample holders using a Horiba Yvon Jobin LabRAM instrument. Measurements were

performed with a 633 nm wavelength laser using ten integrations with a one second acquisition time with a x50 objective and 1800 lines per mm grating.

Magnetometry measurements were performed between 2 K and 300 K both in zero field and an applied field of 1000 Oe using a Magnetic Property Measurement System (MPMS) XL-7 instrument. Hysteresis behaviour was measured in a variable field of ± 70000 Oe with step sizes of 100 Oe (0 – 1000 Oe), 500 Oe (1000 Oe – 5000 Oe) and 5000 Oe (5000 Oe – 70000 Oe) at temperatures of 300 K and 25 K respectively.

Dielectric characterisation was performed on 10 mm pellets, which had been sintered for 3 hours at 850 ^{o}C, using the Agilent 4294A Impedance analyser over a frequency range of approximately 100 Hz – 5 MHz and a temperature range of approximately 50 – 800 K (cooling/heating rates of 2 Kmin^{-1}) and applied excitation of 500 mV. Platinum electrodes were applied to polished pellets using the Emitech K550x sputter coater.

Results and Discussion:

(i) Synchrotron Diffraction

Rietveld refinements were performed for the synchrotron diffraction data collected for $Bi_{1-x}K_xFe_{1-x}Nb_xO_3$ materials with x = 0.0, 0.05, 0.1 and 1.0 using the General Structure Analysis System (GSAS) suite of programs.[1, 2] Initial refinements were performed for the x = 0, 0.05 and 0.1 materials using the *R*3*c* model[3] for approximately 44 variables including 15 background coefficient's fitted using a shifted Chebyschev function and peak shape fitted using a Pseudo-Voigt function. The U*iso* were fixed to 1.00 (Ui/Ue*100), since allowing them to refine resulted in physically unrealistic values, and the fractional occupancies of the atoms not refined. Twelve spherical Harmonic order (ODF) terms were also refined in a cylindrical geometry in order to mitigate against surface roughness effects introduced by preparation of the sample for analysis. In all cases the Texture Index was close to 1 indicating that the sample is randomly orientated. Refinements of the x = 1.0 material were carried using an identical method as described above using the *Amm*2 model.[4] Reitveld refinement parameters and profiles for data collected using powder synchrotron diffraction are presented in tables S1 and figures S1 respectively.

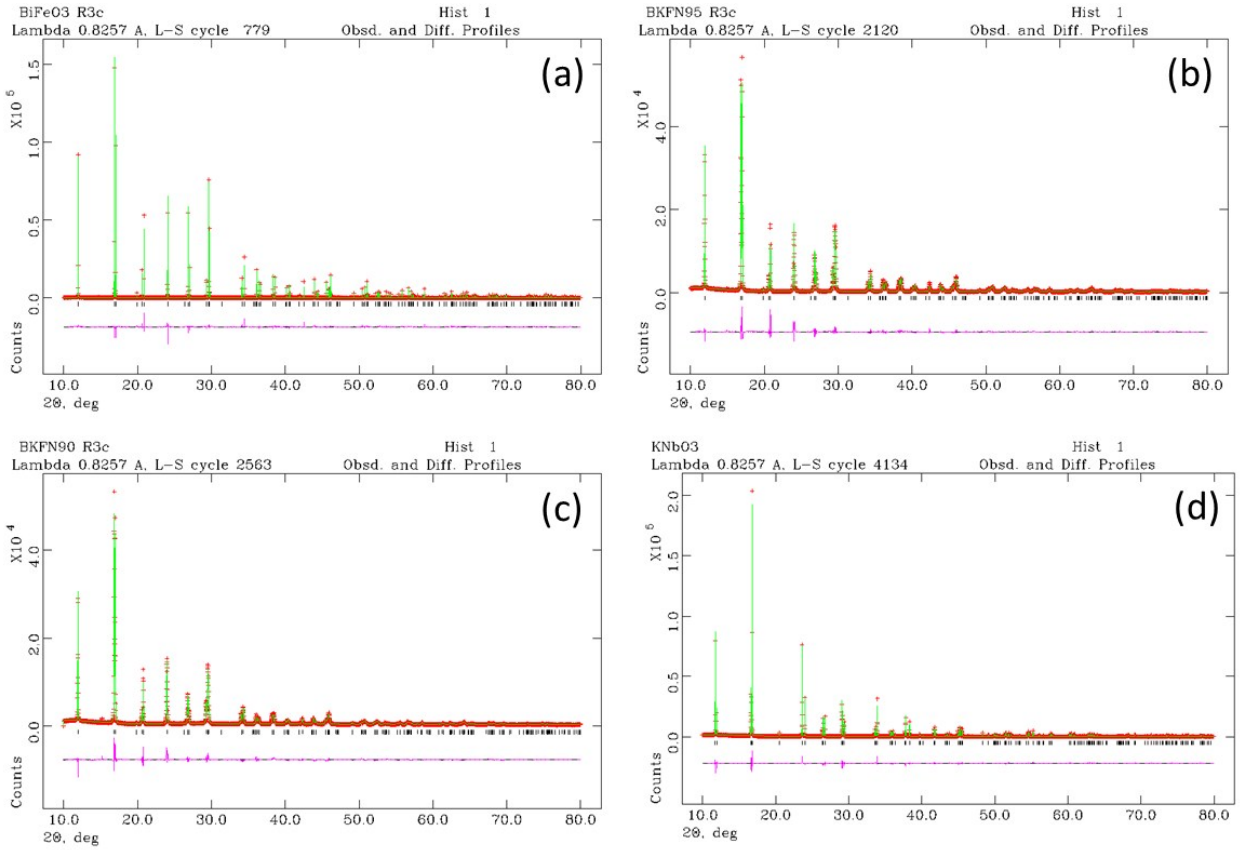

Figure S1: *Rietveld refinement profiles fitted using the R3c[3] ((a) – (c)) and Amm2[4] (d) models for data collected using synchrotron diffraction for (a) $BiFeO_3$, (b) $Bi_{0.95}K_{0.05}Fe_{0.95}Nb_{0.05}O_3$, (c) $Bi_{0.90}K_{0.10}Fe_{0.90}Nb_{0.10}O_3$ and (d) $KNbO_3$. The red circles represent the observed data, the green line represents the calculated model and the pink line represents the difference.*

Table S.3: *Full Rietveld Refinement parameters for data collected for materials in the $Bi_{1-x}K_xFe_{1-x}Nb_xO_3$ with x = 0.0, 0.05, 0.10 and 1.0, using the High Resolution Powder Diffractometer (I11) at the Diamond Light Source. Note: Ui/Ue *100 were fixed to 1.0 and were not refined.*

Parameter		***x* in $Bi_{1-x}K_xFe_{1-x}Nb_xO_3$ materials**			
		0.00	**0.05**	**0.10**	**1.0**
Space group		*R*3*c*	*R*3*c*	*R*3*c*	*Amm*2
χ^2		6.311	10.42	9.439	15.61
wRp (%)		11.56	10.90	10.44	13.72
Rp (%)		8.79	7.75	7.69	9.62
a (Å)		5.571020(3)	5.58862(6)	5.59860(7)	3.97188(1)
b (Å)		5.571020(3)	5.58862(6)	5.59860(7)	5.69347(2)
c (Å)		13.84990(1)	13.8680(2)	13.8655(2)	5.71978(2)
α (º)		90.0	90.0	90.0	90
β (º)		90.0	90.0	90.0	90
γ (º)		120.0	120.0	120.0	90
Cell vol. (Å^3)		372.2603(4)	375.106(8)	376.379(9)	129.3459(8)
Bi/K	***x***	0.0	0.0	0.0	0.0
	y	0.0	0.0	0.0	0.0
	z	0.0	0.0	0.0	0.0113(9)
Fe/ Nb	***x***	0.0	0.0	0.0	0.5
	y	0.0	0.0	0.0	0.0
	z	0.2210(1)	0.2231(2)	0.2256(2)	0.5
O1	***x***	0.443(1)	0.446(2)	0.451(2)	0.0
	y	0.018(2)	0.017633(f)	0.017633(f)	0.0
	z	0.9577(5)	0.9503(8)	0.9492(8)	0.535(2)
O2	***x***	N/A	N/A	N/A	0.5
	y	N/A	N/A	N/A	0.249(2)
	z	N/A	N/A	N/A	0.281(1)
Nb/Fe – O bond length (Å)		2.061(8) 2.061(8) 2.061(8) 1.986(8) 1.986(8) 1.986(8)	2.150(8) 2.150(8) 2.150(8) 1.928(6) 1.928(6) 1.928(6)	2.183(8) 2.183(8) 2.183(8) 1.903(6) 1.903(6) 1.903(6)	1.997(1) 1.997(1) 1.891(9) 1.891(9) 2.151(8) 2.151(8)
Nb/Fe – O – Nb/Fe bond angle (º)		156.2(3)	153.4(5)	153.0(6)	168.4(7) 173.2(6)

(ii) Neutron Diffraction

Powder neutron diffraction refinements were performed for materials between $0.2 \leq x \leq 0.95$ for approximately 27 variables including 15 back ground coefficients fitted in a shifted Chebyschev function and peak shape was fitted using a Pseudo-Voigt function for time-of-flight data. Refinement parameters are given in tables S2 and S3 with the refinement profiles in figures S2 and S3.

Table S.2: *Reitveld Refinement parameters for data collected for materials in the* $Bi_{1-x}K_xFe_{1-x}Nb_xO_3$ *solid solution (between* $0.2 \leq x \leq 0.6$*) using the High Resolution Powder Diffractometer (HRPD) at the ISIS neutron facility. Note only refinement parameters of the main phase are reported.*

Parameter		x in $Bi_{1-x}K_xFe_{1-x}Nb_xO_3$ materials				
		0.2	**0.3**	**0.4**	**0.5**	**0.6**
Space group		*P4mm*	*P4mm*	*P4mm*	*P4mm*	*P4mm*
χ^2		9.466	9.815	5.979	4.418	4.790
wRp (%)		10.27	9.58	7.35	8.23	8.50
Rp (%)		9.26	7.76	5.47	7.31	6.95
a (Å)		3.9883(2)	3.99549(8)	4.00017(6)	4.0045(1)	4.0088(1)
b (Å)		3.9883(2)	3.99549(8)	4.00017(6)	4.0045(1)	4.0088(1)
c (Å)		3.9893(3)	3.9977(1)	4.0020(1)	4.0101(2)	4.0126(3)
α (º)		90	90	90	90	90
β (º)		90	90	90	90	90
γ (º)		90	90	90	90	90
Cell vol. (Å^3)		63.457(6)	63.820(3)	64.038(2)	64.307(4)	64.485(5)
Bi/K	***X***	0.0	0.0	0.0	0.0	0.0
	Y	0.0	0.0	0.0	0.0	0.0
	Z	-0.02(1)	-0.031(8)	-0.021(6)	0.02(1)	0.02(1)
	Ui/Ue *100	9.4(4)	9.9(4)	10.3(2)	8.9(3)	8.27(25)
Fe/Nb	***X***	0.5	0.5	0.5	0.5	0.5
	Y	0.5	0.5	0.5	0.5	0.5
	Z	0.5	0.5	0.5	0.5	0.5
	Ui/Ue *100	1.03(13)	0.87(8)	1.26(3)	1.18(6)	1.27(8)
O1	***X***	0.5	0.5	0.5	0.5	0.5
	Y	0.5	0.5	0.5	0.5	0.5
	Z	-0.001(4)	-0.001(3)	-0.001(3)	0.008(7)	0.012(5)
	Ui/Ue *100	1.83(31)	1.88(29)	2.72(27)	3.29(30)	2.20(33)
O2	***X***	0.5	0.5	0.5	0.5	0.5
	Y	0.0	0.0	0.0	0.0	0.0
	Z	0.558(2)	0.539(2)	0.533(1)	0.529(2)	0.528(2)
	Ui/Ue *100	5.00(37)	3.27(23)	2.65(14)	1.64(12)	1.06(13)
Nb/Fe – O bond length (Å)		1.998(17) 1.991(17) 2.0074(8) 2.0074(8) 2.0074(8) 2.0074(8)	1.994(12) 2.003(12) 2.0037(4) 2.0037(4) 2.0037(4) 2.0037(4)	1.996(12) 2.006(12) 2.0044(3) 2.0044(3) 2.0044(3) 2.0044(3)	1.97(3) 2.04(3) 2.0057(4) 2.0057(4) 2.0057(4) 2.0057(4)	1.96(2) 2.06(2) 2.0075(4) 2.0075(4) 2.0075(4) 2.0075(4)
Nb/Fe – O – Nb/Fe bond angle (º)		180.0(0) 166.8(4)	180.0(0) 171.1(3)	180.0(0) 172.5(2)	180.0(0) 173.3(3)	180.0(0) 173.7(4)
Secondary phase		*R3c*	*R3c*	N/A	N/A	*Amm*2
Secondary Phase %		4.7	2.1	N/A	N/A	9.0

Table S.3: *Rietveld Refinement parameters for data collected for materials in the* $Bi_{1-x}K_xFe_{1-x}Nb_xO_3$ *solid solution (between* $0.6 \leq x \leq 0.95$*) using the High Resolution Powder Diffractometer (HRPD) at the ISIS neutron facility. Note only refinement parameters of the main phase are reported.*

Parameter		***x*** **in** $\mathbf{Bi_{1-x}K_xFe_{1-x}Nb_xO_3}$ **materials**			
		0.70	**0.80**	**0.90**	**0.95**
Space group		*P4mm*	*Amm*2	*Amm*2	*Amm*2
χ^2		2.388	2.150	1.980	2.570
wRp (%)		5.99	5.90	5.98	6.54
Rp (%)		5.81	6.01	5.96	6.28
a (Å)		4.0093(1)	4.0147(3)	4.0208(3)	4.0266(2)
b (Å)		4.0093(1)	5.6698(5)	5.6699(6)	5.6708(4)
c (Å)		4.0145(2)	5.6742(2)	5.6727(2)	5.6686(2)
α (º)		90	90	90	90
β (º)		90	90	90	90
γ (º)		90	90	90	90
Cell vol. (Å³)		64.540(4)	129.16(2)	129.32(2)	129.44(1)
Bi/K	***x***	0.0	0.0	0.0	0.0
	y	0.0	0.0	0.0	0.0
	z	0.01(1)	-0.024(4)	-0.029(2)	-0.029(2)
	Ui/Ue *100	6.18(13)	3.02(22)	0.55(11)	-0.09(11)
Fe/Nb	***x***	0.5	0.5	0.5	0.5
	y	0.5	0.0	0.0	0.0
	z	0.5	0.5	0.5	0.5
	Ui/Ue *100	1.08(8)	1.18(8)	0.87(6)	1.17(5)
O1	***x***	0.5	0.0	0.0	0.0
	y	0.5	0.0	0.0	0.0
	z	0.016(4)	0.495(3)	0.485(2)	0.488(2)
	Ui/Ue *100	1.87(25)	1.45(24)	0.48(24)	0.35(16)
O2	***x***	0.5	0.5	0.5	0.5
	y	0.0	0.234(1)	0.234(1)	0.233(1)
	z	0.528(1)	0.239(2)	0.245 (2)	0.250(1)
	Ui/Ue *100	0.79(10)	0.65(9)	0.43(13)	0.57(10)
Nb/Fe – O bond length (Å)		1.94(2) 2.07(2) 2.0079(4) 2.0079(4) 2.0079(4) 2.0079(4)	2.0075(3) 2.0075(3) 1.989(13) 1.989(13) 2.028(12) 2.028(12)	2.0122(5) 2.0122(5) 1.962(8) 1.962(8) 2.052(8) 2.052(8)	2.0146(4) 2.0146(4) 1.938(7) 1.938(7) 2.074(7) 2.074(7)
Nb/Fe – O – Nb/Fe bond angle (º)		180.0(0) 173.5(4)	178.5(11) 173.9(4)	175.1(6) 175.2(4)	176.0(6) 175.9(4)
Secondary phase		*Amm*2	N/A	N/A	N/A
Secondary Phase %		9.2	N/A	N/A	N/A

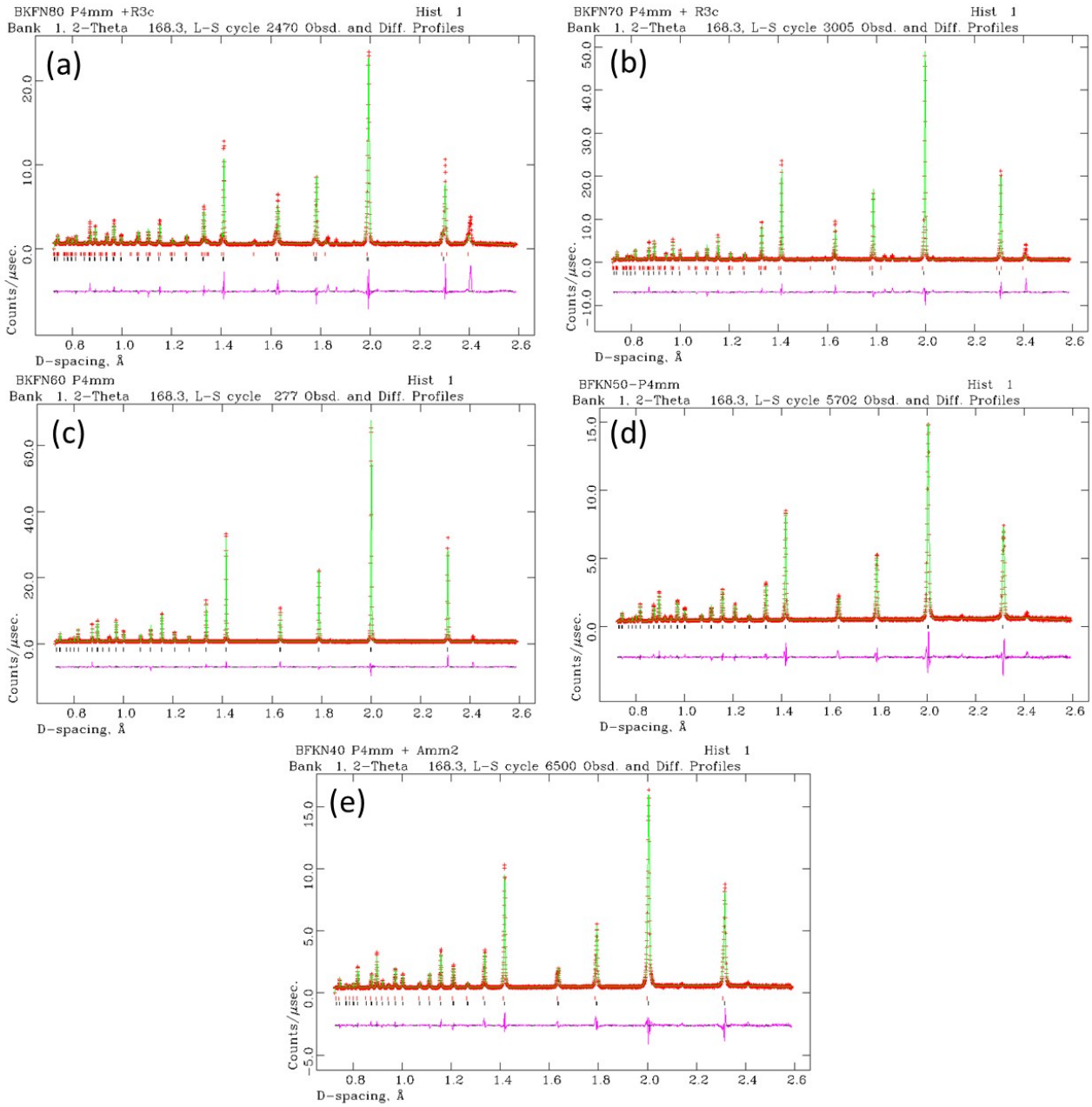

Figure S2: *Rietveld refinement profiles fitted using the P4mm,[4] R3c[3] and Amm2[4] models for data collected using neutron diffraction for (a) $Bi_{0.80}K_{0.20}Fe_{0.80}Nb_{0.20}O_3$ (b) $Bi_{0.70}K_{0.30}Fe_{0.70}Nb_{0.30}O_3$, (c) $Bi_{0.60}K_{0.40}Fe_{0.60}Nb_{0.40}O_3$, (d) $Bi_{0.50}K_{0.50}Fe_{0.50}Nb_{0.50}O_3$ and (e) $Bi_{0.40}K_{0.60}Fe_{0.40}Nb_{0.60}O_3$. The red circles represent the observed data, the green line represents the calculated model and the pink line represents the difference. Black and red tick marks represent the P4mm and R3c models in (a) and (b) and P4mm and Amm2 models in (e) respectively.*

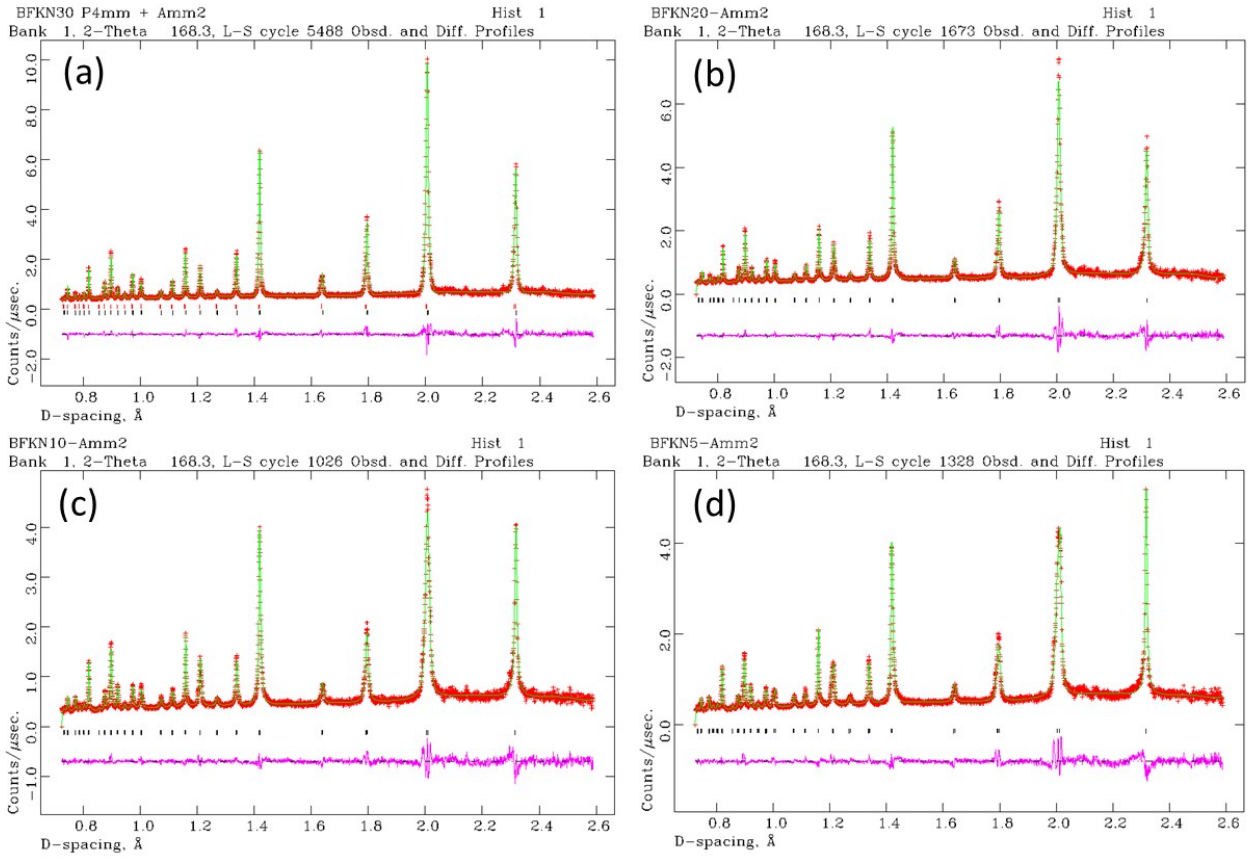

Figure S3: *Rietveld refinement profiles fitted using the P4mm[4] (a) and Amm2[4] ((b) – (c)) models for data collected using neutron diffraction for (a) $Bi_{0.30}K_{0.70}Fe_{0.30}Nb_{0.70}O_3$ (b) $Bi_{0.20}K_{0.80}Fe_{0.20}Nb_{0.80}O_3$, (c) $Bi_{0.10}K_{0.90}Fe_{0.10}Nb_{0.90}O_3$ and (d) $Bi_{0.05}K_{0.95}Fe_{0.0.05}Nb_{0.95}O_3$. The red circles represent the observed data, the green line represents the calculated model and the pink line represents the difference. Black and red tick marks represent the P4mm and and Amm2 models in (a) respectively.*

Table S.3: *Table of pseudo-cubic lattice parameters, cell volume and tetragonality. P4mm* exhibits a straight forward relationship with the aroistotype cubic cell with a $a_{tet} = a_{cub}$, and $c_{tet} = a_{cub}$ setting; for *Amm*2 the lattice parameters can be related through a $a_{orth} = a_{cub}$, $b_{orth} = \sqrt{2}a_{cub}$ and $c_{orth} = \sqrt{2}a_{cub}$ relationship

Composition, x	**Symmetry**	$a_{tet/orth}$ **(Å)**	a_{cub} **(Å)**	$b_{tet/orth}$ **(Å)**	b_{cub} **(Å)**	$c_{tet/orth}$ **(Å)**	c_{cub} **(Å)**	**Pseudo-cubic cell volume (Å³)**	**Tetragonality (*c*/*a*)**
0.2	*P4mm*	3.9883	3.9883	3.9883	3.9883	3.9893	3.9893	63.45595	1.000251
0.3	*P4mm*	3.99549	3.99549	3.99549	3.99549	3.9977	3.9977	63.81904	1.000553
0.4	*P4mm*	4.00017	4.00017	4.00017	4.00017	4.002	4.002	64.03744	1.000457
0.5	*P4mm*	4.0045	4.0045	4.0045	4.0045	4.0101	4.0101	64.30604	1.001398
0.6	*P4mm*	4.0088	4.0088	4.0088	4.0088	4.0126	4.0126	64.4844	1.000948
0.7	*P4mm*	4.0093	4.0093	4.0093	4.0093	4.0145	4.0145	64.53103	1.001297
0.8	*Amm*2	4.0147	4.0147	5.6698	4.009154	5.6742	4.012265	64.57962	0.999394
0.9	*Amm*2	4.0208	4.0208	5.6699	4.009225	5.6727	4.011205	64.66179	0.997614
0.95	*Amm*2	4.0266	4.0266	5.6686	4.008306	5.6708	4.009861	64.71853	0.995843

(iii) X-ray Fluorescence Spectroscopy

Table S4 gives a table of the calculated and expected phase fractions (by mass) for these materials as determined by XRF spectroscopy. In these measurements calibrations were performed taking into account the expected stoichiometry of the parent $BiFeO_3$ and $KNbO_3$ materials. With the exception of $x = 0.2$ all analysis were within 1 – 2 % of the expected values confirming the trends observed in the diffraction data. The values for the $x = 0.2$ material were closer to an approximate error of 3 % which may suggest that this material is slightly off stoichiometry.

Table S.4: *Table of calculated and expected compositions (by mass) from x-ray fluorescence spectroscopy for the* $Bi_{1-x}K_xFe_{1-x}Nb_xO_3$ *materials.*

x in $Bi_{1-x}K_xFe_{1-x}Nb_xO_3$	Bi		K		FeO_3		Nb	
	Calc.	Exp.	Calc.	Exp.	Calc.	Exp.	Calc.	Exp.
0.1	63.8	65.1	1.3	1.3	31.7	30.4	3.2	3.2
0.2	60.4	63.3	2.8	2.1	30.0	28.1	6.7	6.5
0.3	56.6	57.8	4.5	4.4	28.1	27.7	10.8	10.1
0.4	52.1	54.5	6.5	5.5	25.9	26.4	15.5	13.6
0.5	47.0	46.4	8.8	9.2	23.3	23.6	20.9	20.8
0.6	40.9	40.2	11.5	11.5	20.3	20.4	27.3	28.0
0.7	33.7	34.8	14.7	15.7	16.7	17.1	34.9	32.5
0.8	24.9	25.6	18.6	20.1	12.3	12.5	44.2	41.7
0.9	13.9	14.2	23.4	28.3	6.9	6.9	55.7	50.6
0.95	7.4	8.7	26.3	29.9	3.7	4.2	62.6	57.5

(iv) Raman Analysis

Figures S4 and S5 give the Raman spectra collected for $BiFeO_3$ and $KNbO_3$, and the $Bi_{1-x}K_xFe_{1-x}Nb_xO_3$ materials in the composition range $0.0 \leq x \leq 1.0$ respectively.

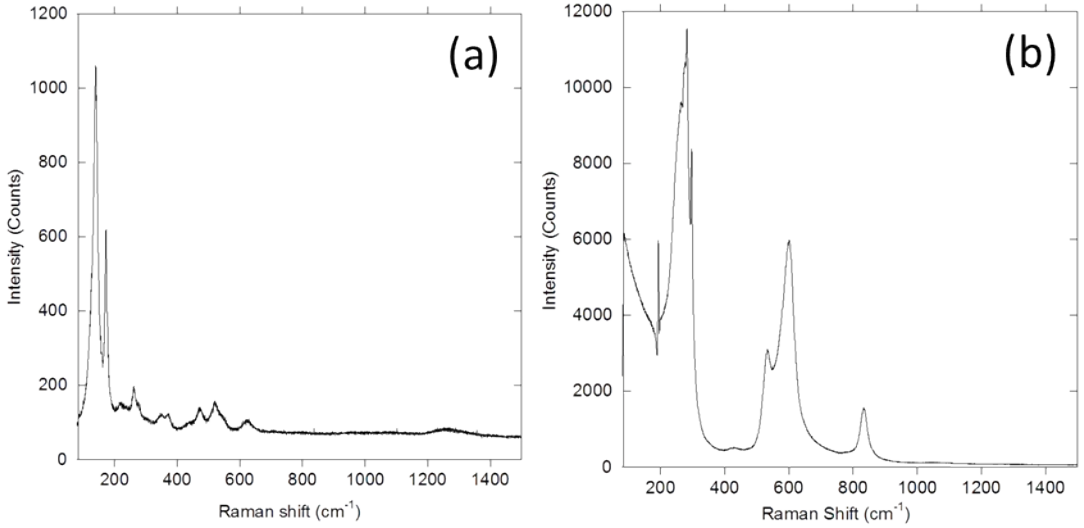

Figure S4: *Raman spectra collected at room temperature for (a) $BiFeO_3$ and (b) $KNbO_3$.*

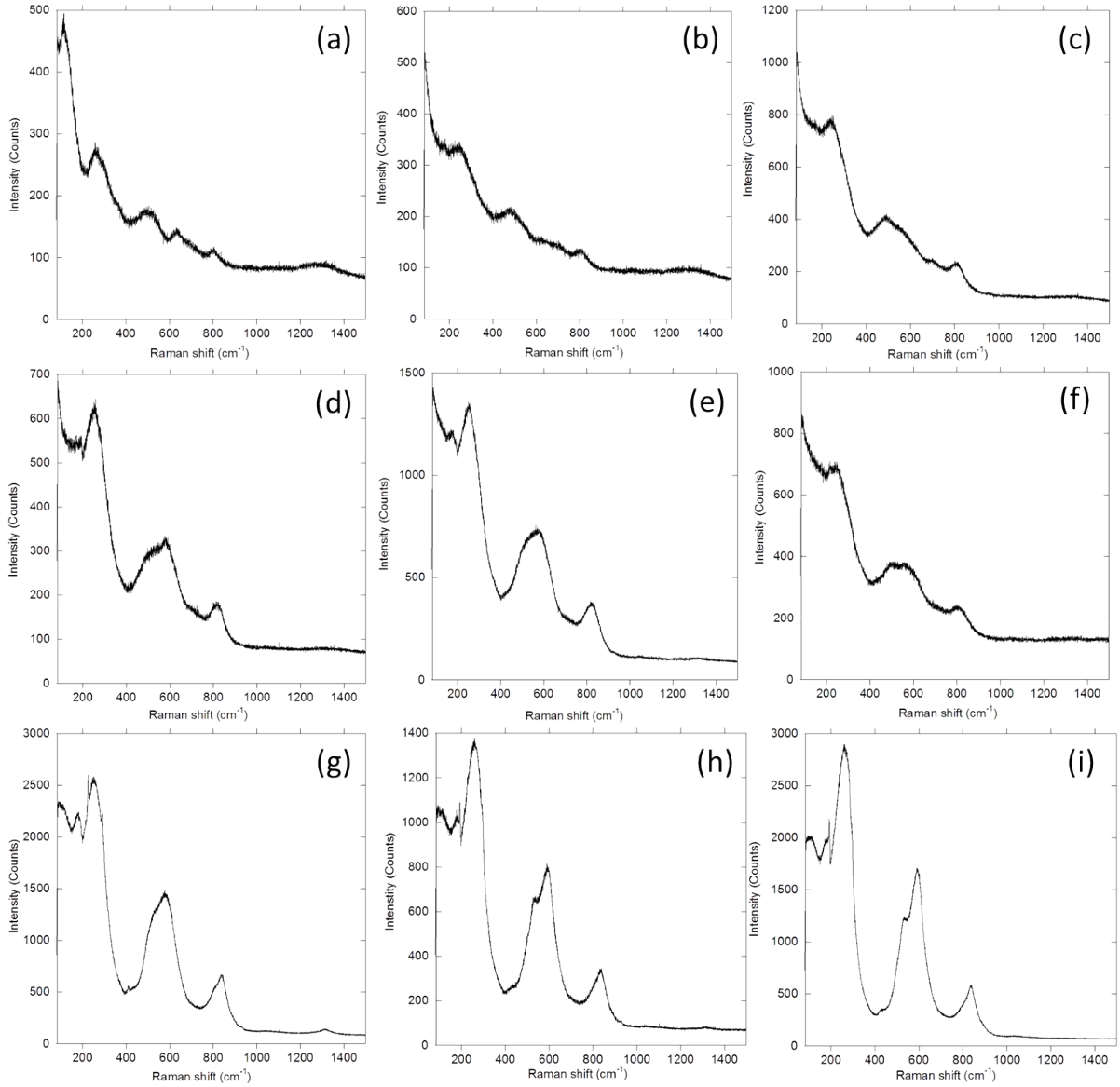

(v) ***Figure S4:*** *Raman spectra collected at room temperature for (a)* $Bi_{0.90}K_{0.10}Fe_{0.90}Nb_{0.10}O_3$ *(b)* $Bi_{0.80}K_{0.20}Fe_{0.80}Nb_{0.20}O_3$*, (c)* $Bi_{0.70}K_{0.30}Fe_{0.70}Nb_{0.30}O_3$*, (d)* $Bi_{0.60}K_{0.40}Fe_{0.60}Nb_{0.40}O_3$*, (e)* $Bi_{0.50}K_{0.50}Fe_{0.50}Nb_{0.50}O_3$*, (f)* $Bi_{0.40}K_{0.60}Fe_{0.40}Nb_{0.60}O_3$*, (g)* $Bi_{0.30}K_{0.70}Fe_{0.30}Nb_{0.70}O_3$*, (h)* $Bi_{0.20}K_{0.80}Fe_{0.20}Nb_{0.80}O_3$ *and (i)* $Bi_{0.10}K_{0.90}Fe_{0.10}Nb_{0.90}O_3$*.* Magnetometer Data

Figures S5 through S8 give variable temperature zero field cooled (ZFC) and field cooled (FC) data and magnetisation-field curves collected for $Bi_{1-x}K_xFe_{1-x}Nb_xO_3$ materials with compositions in $x = 0.1$ increments.

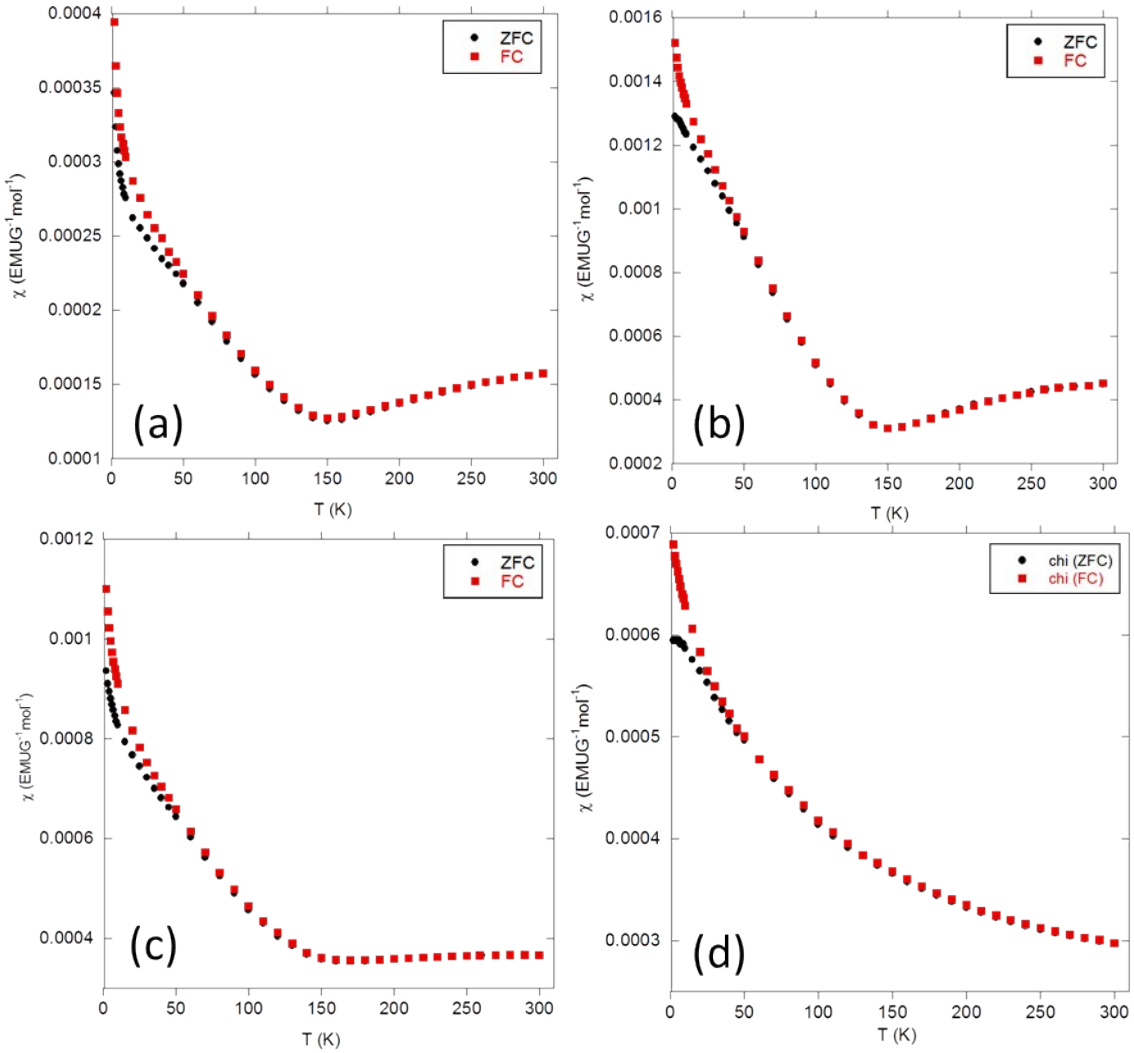

Figure S5: *Variable temperature zero field cooled (ZFC) and field cooled (FC) SQUID magnetometry data collected for (a)* $Bi_{0.90}K_{0.10}Fe_{0.90}Nb_{0.10}O_3$ *(b)* $Bi_{0.80}K_{0.20}Fe_{0.80}Nb_{0.20}O_3$*, (c)* $Bi_{0.70}K_{0.30}Fe_{0.70}Nb_{0.30}O_3$ *and (d)* $Bi_{0.60}K_{0.40}Fe_{0.60}Nb_{0.40}O_3$*.*

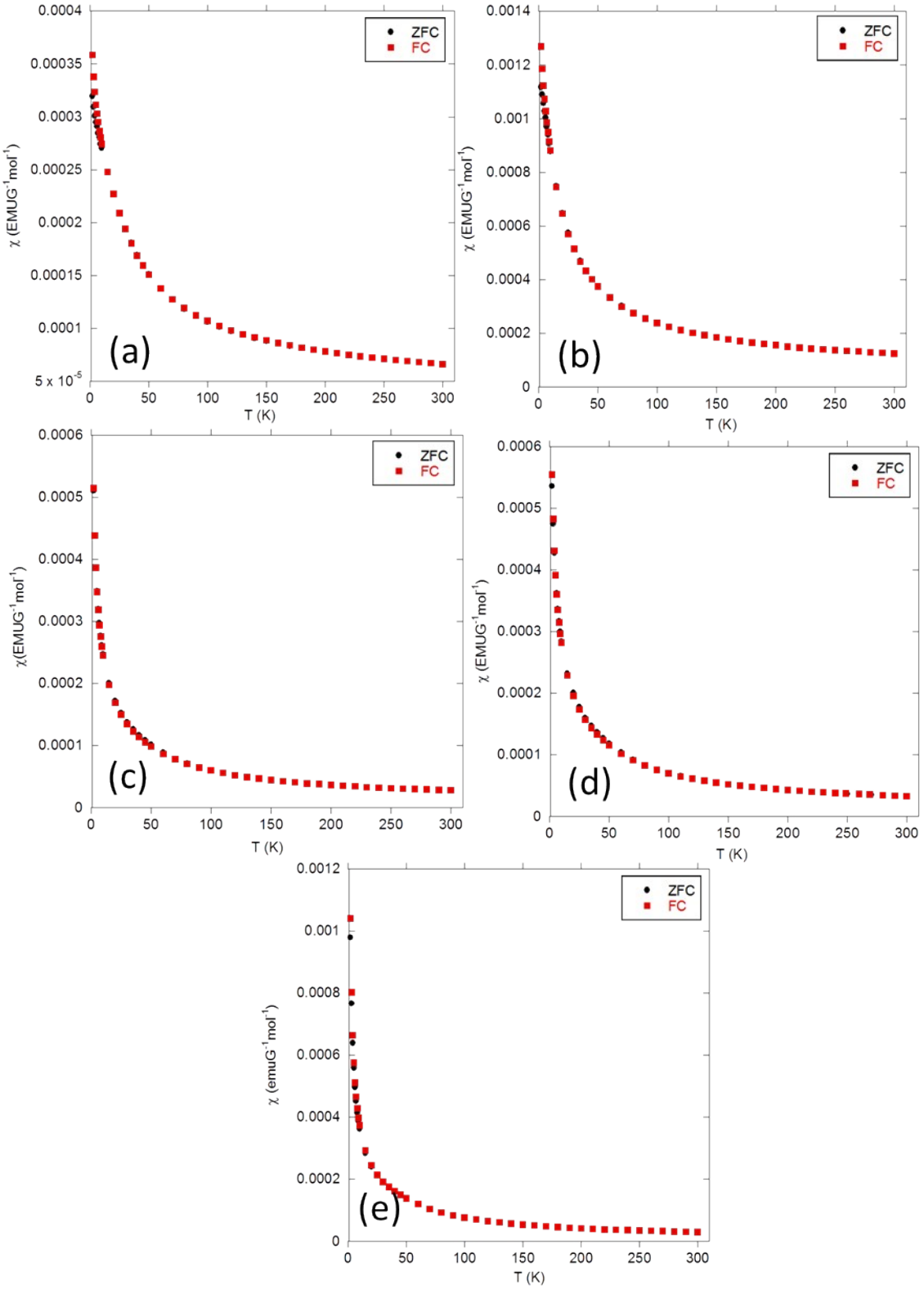

Figure S6: *Variable temperature zero field cooled (ZFC) and field cooled (FC) SQUID magnetometry data collected for (a)* $Bi_{0.50}K_{0.50}Fe_{0.50}Nb_{0.50}O_3$*, (b)* $Bi_{0.40}K_{0.60}Fe_{0.40}Nb_{0.60}O_3$*, (c)* $Bi_{0.30}K_{0.70}Fe_{0.30}Nb_{0.70}O_3$*, (d)* $Bi_{0.20}K_{0.80}Fe_{0.20}Nb_{0.80}O_3$ *and (e)* $Bi_{0.10}K_{0.90}Fe_{0.10}Nb_{0.90}O_3$*.*

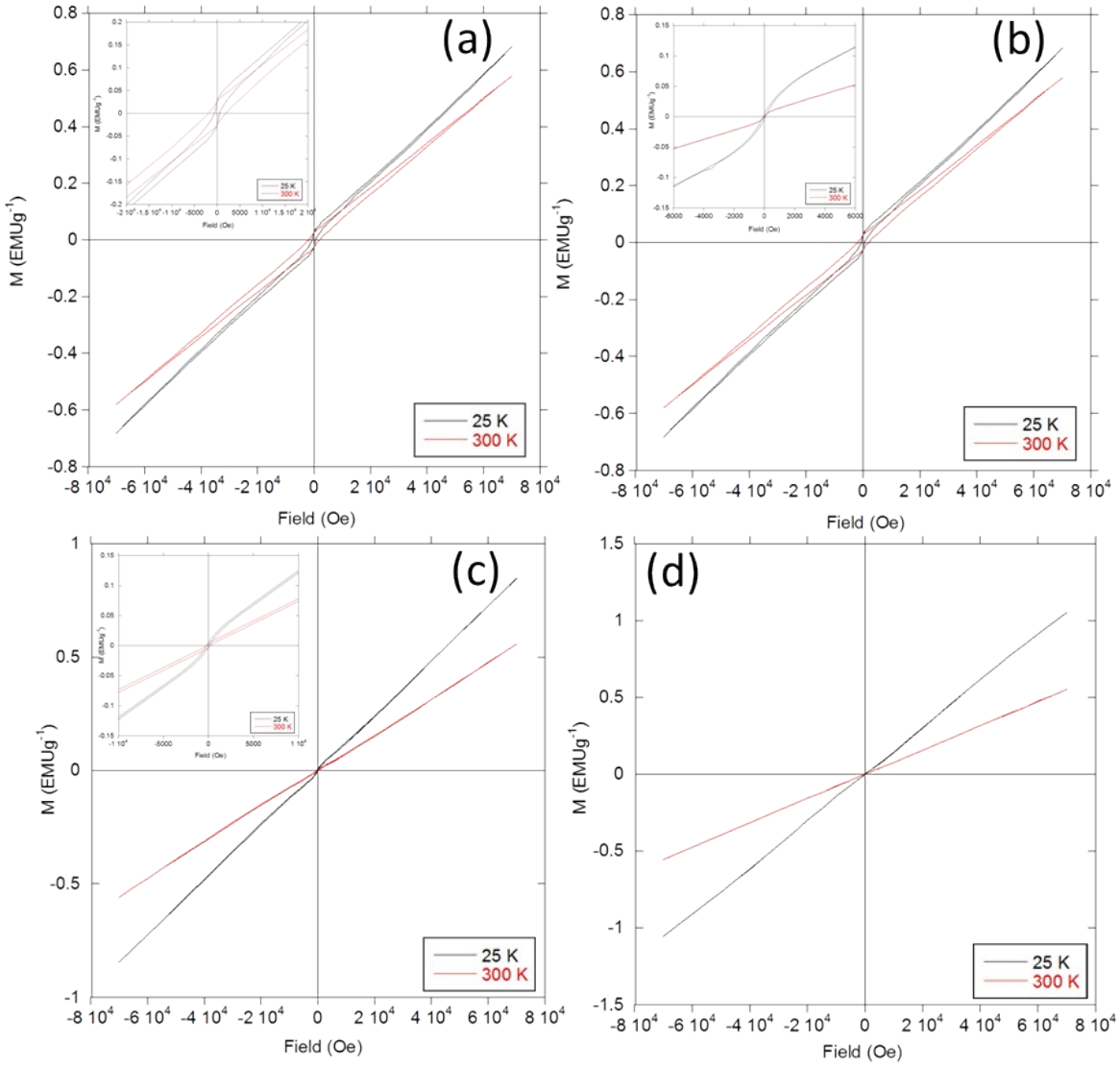

Figure S7: *Magnetization-field curves collected at 300 K and 25 K for (a)* $Bi_{0.90}K_{0.10}Fe_{0.90}Nb_{0.10}O_3$ *(b)* $Bi_{0.80}K_{0.20}Fe_{0.80}Nb_{0.20}O_3$*, (c)* $Bi_{0.70}K_{0.30}Fe_{0.70}Nb_{0.30}O_3$ *and (d)* $Bi_{0.60}K_{0.40}Fe_{0.60}Nb_{0.40}O_3$*. Insets in (a), (b) and (c) show zoomed in regions of the curves indicating hysteric behaviour at both 300 K and 25 K.*

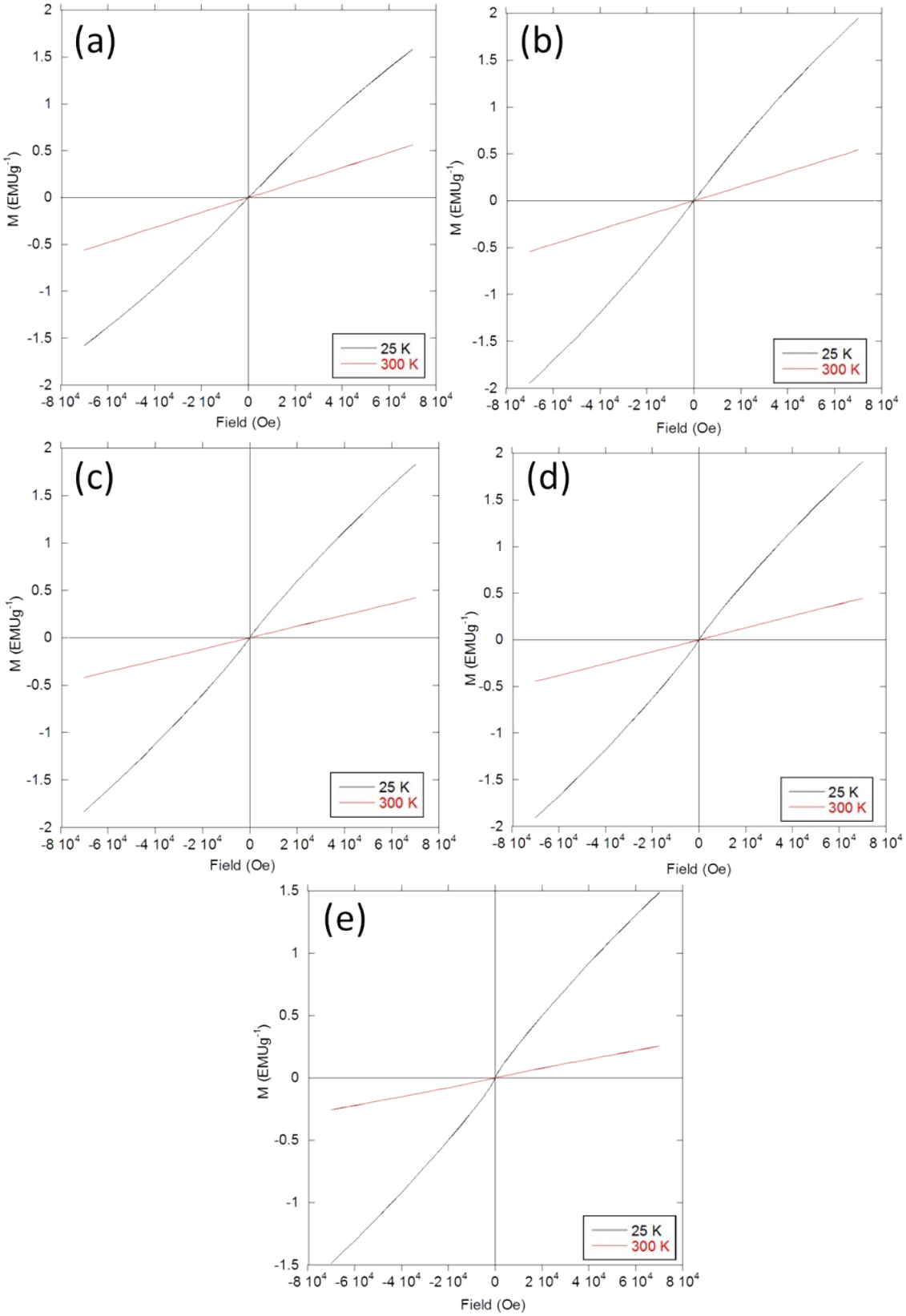

Figure S8: *Magnetization-field curves collected at 300 K and 25 K for (a) $Bi_{0.50}K_{0.50}Fe_{0.50}Nb_{0.50}O_3$, (b) $Bi_{0.40}K_{0.60}Fe_{0.40}Nb_{0.60}O_3$, (c) $Bi_{0.30}K_{0.70}Fe_{0.30}Nb_{0.70}O_3$, (d) $Bi_{0.20}K_{0.80}Fe_{0.20}Nb_{0.80}O_3$ and (e) $Bi_{0.10}K_{0.90}Fe_{0.10}Nb_{0.90}O_3$.*

(vi) Electrical Data

Figure S9 gives variable temperature vs. dielectric constant data for $Bi_{1-x}K_xFe_{1-x}Nb_xO_3$ materials with compositions in x = 0.1, 0.2, 0.3, 0.4, 0.5 and 0.8. It was not possible to prepare dense pellets of the remaining compositions in this current study. In all cases the materials showed frequency dependent high permittivity behaviour characteristic of non-ohmic electrode effects arising from 'leaky' dielectrics making it difficult to extract meaningful information.

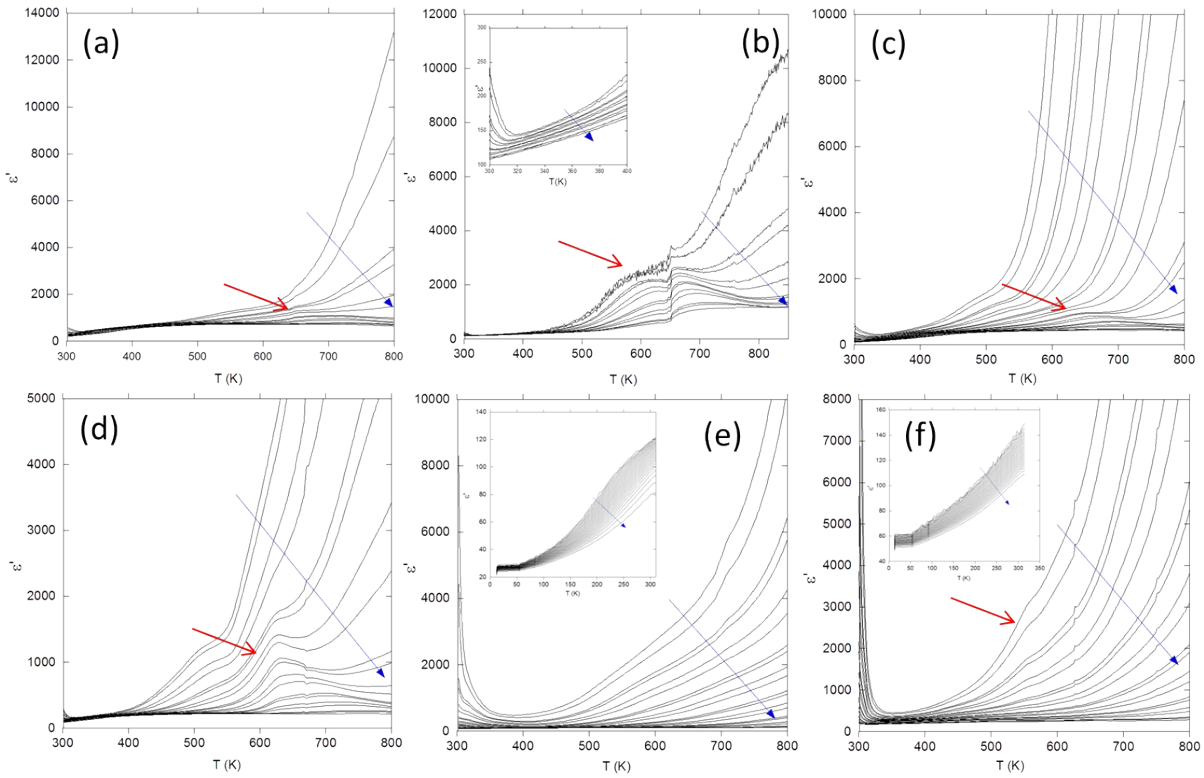

Figure S9: *Dielectric constant vs. temperature data for (a)* $Bi_{0.90}K_{0.10}Fe_{0.90}Nb_{0.10}O_3$ *(b)* $Bi_{0.80}K_{0.20}Fe_{0.80}Nb_{0.20}O_3$, *(c)* $Bi_{0.70}K_{0.30}Fe_{0.70}Nb_{0.30}O_3$, *(d)* $Bi_{0.60}K_{0.40}Fe_{0.60}Nb_{0.40}O_3$, *(e)* $Bi_{0.50}K_{0.50}Fe_{0.50}Nb_{0.50}O_3$, *and (f)* $Bi_{0.20}K_{0.80}Fe_{0.20}Nb_{0.80}O_3$. *Inset in figure (b) shows a zoomed in region close to room temperature inidicating the frequency dependent anomaly at room temperature. The inset of figures (e) and (f) show low temperature data which suggests a potential transition close to room temperature. Note the low temperature data collected for materials (a), (b), (c) and (d) did not show anything of interest. The red arrows highlight anomalies observed in the data between 500 K and 600 K and the blue arrows indicate increasing frequency.*

References

1. C. Larson and R. B. V. Dreele, *Los Alamos National Laboratory Report LAUR,* **96**, *86*.
2. H. Toby, *J. Appl. Cryst.* **2001**, *34*, 210.
3. D. C. Arnold, K. S. Knight, F. D. Morrison and P. Lightfoot, *Phys. Rev. Lett.*, **2009**, *102*, 027602
4. A. W. Hewat, *J. Phys. C.*, **1973**, *6*, 2559